Journal of Solid State Chemistry **154,** 168–176 (2000)
doi:10.1006/jssc.2000.8831, available online at http://www.idealibrary.com on IDEAL®

Crystal Chemistry of α-AlB_{12} and γ-AlB_{12}

Iwami Higashi

Department of Chemistry, Chiba Institute of Technology, Shibazono, Narashino, Chiba 275-0023, Japan

Received September 9, 1999; in revised form February 18, 2000; accepted February 28, 2000

The structures of α-AlB_{12} and γ-AlB_{12} are both characterized by a rigid boron framework derived from a combination of three-dimensional networks of icoasahedral B_{12} and B_{20} units. Crystals of γ-AlB_{12} ($P2_12_12$; $a = 16.57$, $b = 17.51$, $c = 10.14$ Å) are almost always obtained as syntactically intergrown crystals with α-AlB_{12} ($P4_12_12$ or $P4_32_12$; $a = 10.16$, $c = 14.27$Å) from high-temperature Al–B solutions. Examination of structural details of α-AlB_{12} and γ-AlB_{12} demonstrated that there are close similarities between them, notwithstanding marked differences in the crystal data. The syntactic intergrowth between α-AlB_{12} and γ-AlB_{12} is always effected so as to have the $(101)_\alpha$ and the $(100)_\gamma$ planes parallel to each other and the a_α or b_α axis and the c_γ axis in the same direction; these planes are identical in unit area and in the orientation inside the intergrown crystals. This fact, as well as the fact that the icosahedral B_{12} networks of both crystals which are parallel to the syntactic intergrowth plane are identical, may facilitate the formation of the intergrown crystal. Structural details of one crystal are compared to the corresponding ones of the other. © 2000 Academic Press

1. INTRODUCTION

At present in the binary Al–B system only three phases, AlB_2 (1), α-AlB_{12} (2, 3), and (with less confidence) γ-AlB_{12} (3), are considered to be pure binary aluminum borides. The phases AlB_{10} (4) and β-AlB_{12} (2) were shown to be ternary compounds containing carbon. It was reported by Matkovich *et al.* (5) that γ-AlB_{12} could not be prepared as single crystals but as intergrown crystals with α-AlB_{12}.

By use of high-temperature Al–B solution growth methods or by sintering powdery Al–B compacts (6), we have also collaborated that as for boron-rich compounds only α-AlB_{12} and γ-AlB_{12} could be prepared, and these two boron-rich phases are always obtained as sintactically intergrown crystals as had been reported by Kohn and Eckart (3). Furthermore, our extensive efforts (6) to find a reproducible method to prepare the single phase or single crystals of γ-AlB_{12}, which eventually proved to be in vain, showed the somewhat unstable nature of this phase; when the intergrown crystals are pulverized to prepare a sample for powder X-ray diffraction, the γ-AlB_{12} phase is entirely transformed into the α-AlB_{12} phase (6). Single-phase crystals of the γ-AlB_{12} structure type doped with Mg ($Al_{1.4}Mg_{0.5}B_{22}$), which are obtainable by cooling a high-temperature Al–B solution containing a small quantity of Mg, however, cannot be transformed into the α-AlB_{12} structure type by pulverization (6). Crystal data for α-AlB_{12}, and γ-AlB_{12} phases are presented in Table 1.

The α-AlB_{12} phase was prepared as pure binary crystals by cooling Al–B melts from temperatures of about 1500°C, and its structure determined by the single-crystal X-ray diffractometry (8, 9). Since the structure analysis of γ-AlB_{12} was done by using the γ-AlB_{12} crystals which had been prepared by the same method as for the α-AlB_{12} phase (possibly at slightly lower temperatures) (10, 11), it would be highly probable that the crystals used for the X-ray diffraction work had contained a small quantity of Mg or certain other impurity atoms. From this context, it is of interest to point out that one set of the published data ($a = 16.623(5)$, $b = 17.540(5)$, $c = 10.180(5)$ Å) of the γ-AlB_{12} single crystal utilized for the structure determination (10) is almost the same as those of the $Al_{1.4}Mg_{0.5}B_{22}$ crystal of the γ-AlB_{12} structure type (7), although they are significantly different from those for another γ-AlB_{12} crystal (11) (see Table 1); the latter had been found by chance among a large amount of the intergrown crystals of α-AlB_{12} and γ-AlB_{12} (12). Although there are significant differences in the metal distribution, the results from three publications (7, 10, 11) from which the crystal data are cited in the Table 1 were all the same with regard to the structure of born framework.

In the present paper structural details of boron frameworks in the α-AlB_{12} and the γ-AlB_{12} structures are described, demonstrating that there are close similarities between the two structures, notwithstanding a great difference in the crystal data (Table 1).

2. DESCRIPTIONS OF STRUCTURES

Structural data are available from Refs. (8 and 9) for α-AlB_{12} and from Refs. (10 and 11) for γ-AlB_{12}. Although the structures of α-AlB_{12} (8) and γ-AlB_{12} (11) have been described in detail, some of their general features will be given

0022-4596/00 $35.00

TABLE 1
Crystal Data for the Crystals of α-AlB_{12} and γ-AlB_{12} Structure Type

Crystal	α-AlB_{12}	γ-AlB_{12}	γ-AlB_{12}	$Al_{1.4}Mg_{0.5}B_{22}$[a]
Crystal system	Tetragonal		Orhorhombic	
a (Å)	10.158(2)	16.573(4)	16.623(5)	16.633(3)
b (Å)	(= *a*)	17.510(3)	17.540(5)	17.547(4)
c (Å)	14.270(5)	10.144(1)	10.180(5)	10.187(2)
Chemical formula[b]	$B_{22}Al_{1.6}$	$B_{88}Al_{6.3}$	$B_{88}Al_{6.5}$	$B_{88}Al_{5.6}Mg_2$
Reference	8	11	10	7

[a] γ-AlB_{12} structure type.

[b] Asymmetric units determined by x-ray structure analysis; expressed in terms of boron structural subunits, they are 1/2 $(2B_{12} \cdot B_{20}(I))$ and $B_{12}(I) \cdot B_{12}(II) \cdot B_{12}(III) \cdot B_{12}(IV) \cdot B_{20}(I) \cdot B_{20}(II)$ for α-AlB_{12} and γ-AlB_{12} structure type, respectively.

here to facilitate discussions. There are three main components of the structures of α-AlB_{12} and γ-AlB_{12}: (i) arrangements of icosahedral B_{12} units; (ii) arrangement of B_{20} units; and (iii) statistical distribution of metal atoms in the boron framework. The B_{20} unit is a twinned icosahedron with a B–B–B triangular composition plane. It has two vacant apical sites and an isolated B atom bridging both sides of the unit. There are two types of B_{20} unit; stereoscopic views of them are presented in Figs. 1 and 2. One of the B_{20} units, B_{20}-(C_2), having one vacant site at each side of the unit (Fig. 1), is that which is present in the α-AlB_{12} structure, and the other, B_{20}-(C_s), having two vacant sites at one side of the unit (Fig. 2), is the one that has been found only in γ-AlB_{12}; in the γ-AlB_{12} structure both types of B_{20} units are present (10). Each of the symbols characterizes the symmetry of the unit in the standard Schoenflies notation (10). In earlier papers, the B_{20} unit in α-AlB_{12} (8, 9) and the B_{22} unit in β-tetragonal boron (13) were referred to as the B_{19} unit and the B_{21} unit, respectively, excluding the isolated B atom bridging both sides of the twinned icosahedron; the B_{22} unit is identical with the B_{20} unit except that it has no vacant apical site. From an electronic point of view (11, 14, 15), however, the superficially isolated single B atom bridging two sides of each of the units is regarded as an additional member of the twinned icosahedron units (16).

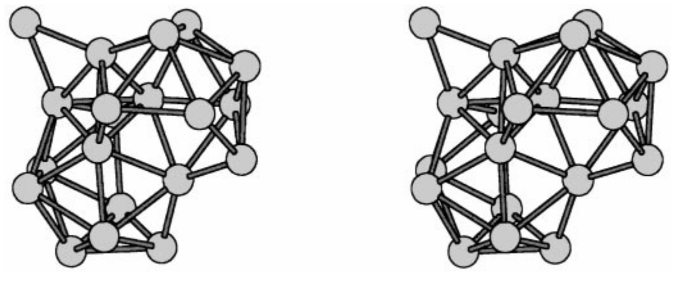

FIG. 1. Stereoscopic view of B_{20}-(C_2) unit.

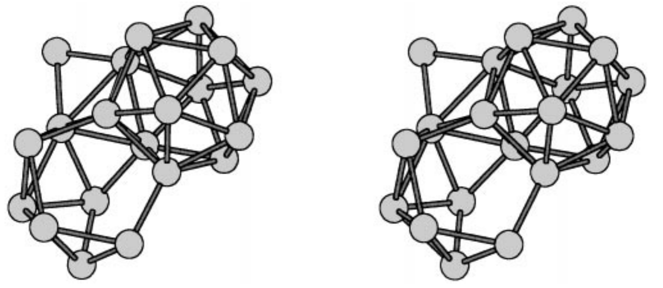

FIG. 2. Stereoscopic view of B_{20}-(C_s) unit.

In the structures of both α-AlB_{12} and γ-AlB_{12}, the linkages of B_{12}–B_{12}, B_{12}–B_{20}, and B_{20}–B_{20} are effected through quasi-fivefold axes of B_{12} icosahedra and similar directions of the B_{20} units.

2.1. α-AlB_{12}

The structure of α-AlB_{12} (8, 9) is characterized by the presence of an icosahedral B_{12} framework (Fig. 3) combined with that of B_{20} units (Fig. 4). As mentioned above, the B_{20} units in the α-AlB_{12} structure are of the B_{20}-(C_2) type. The arrangement of B_{12} icosahedra as presented in Fig. 3 is described as an alternate alignment of icosahedral B_{12} chains running along the *a* and *b* axes; the alternate alignment is generated by the operation of the 4_1 or 4_3 screw axis (of the space group $P4_12_12$ or $P4_32_12$), which results in the construction of a rigid three-dimensional icosahedral B_{12} framework having large openings capable of accommodating B_{20} units. By rephrasing icosahedral B_{12} chains with zigzag chains of B_{20} units, a similar description can be made regarding the construction of a rigid framework of B_{20} units (Fig. 4). The nature of the coordination of B_{12} icosahedra about the B_{20} unit is the same as that in the γ-AlB_{12} structure, which will be described below. The α-AlB_{12} phase decomposes by arc melting, expelling the Al metal to form a solid solution of the β-rhombohedral boron structure with a composition of AlB_{31} (17); the decomposition temperature is around 2000°C (3, 18).

2.2. γ-AlB_{12}

As shown in Table 1, the asymmetric unit of boron in γ-AlB_{12} consists of four crystallographycally independent B_{12} icosahedra, B_{20}-(C_2), and B_{20}-(C_s); on the other hand, that in α-AlB_{12} is $1/2(2B_{12} \cdot B_{20})$. As in the case of the α-AlB_{12} structure, the structure of γ-AlB_{12} is also characterized by the presence of an icosahedral B_{12} framework combined with that of B_{20} units. An icosahedral B_{12} network as

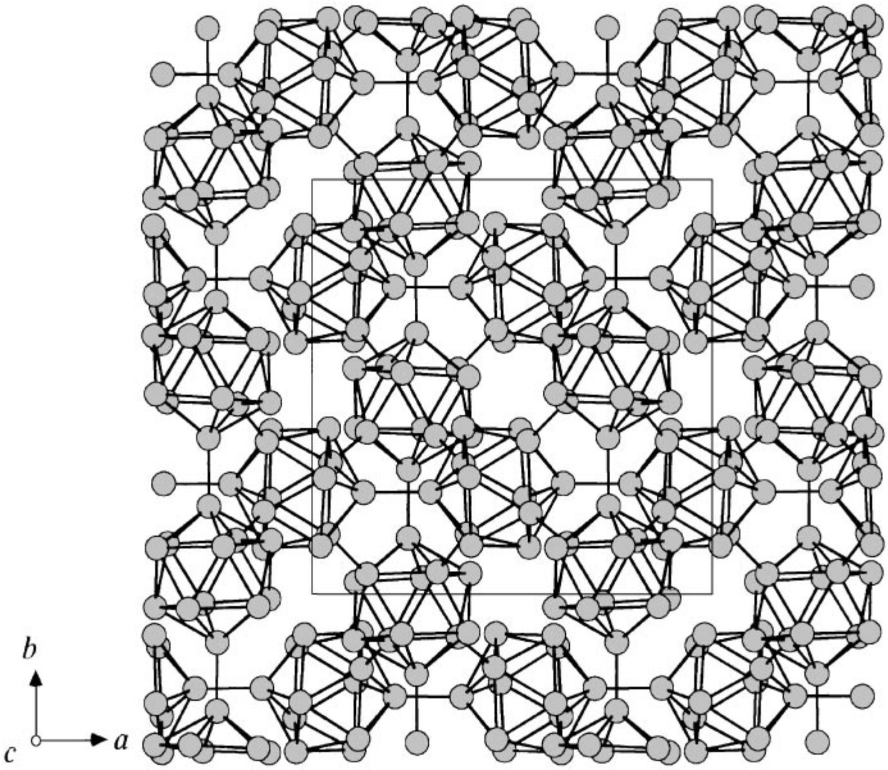

FIG. 3. Arrangement of B_{12} icosahedra in the α-AlB_{12} structure as seen along the *c* axis.

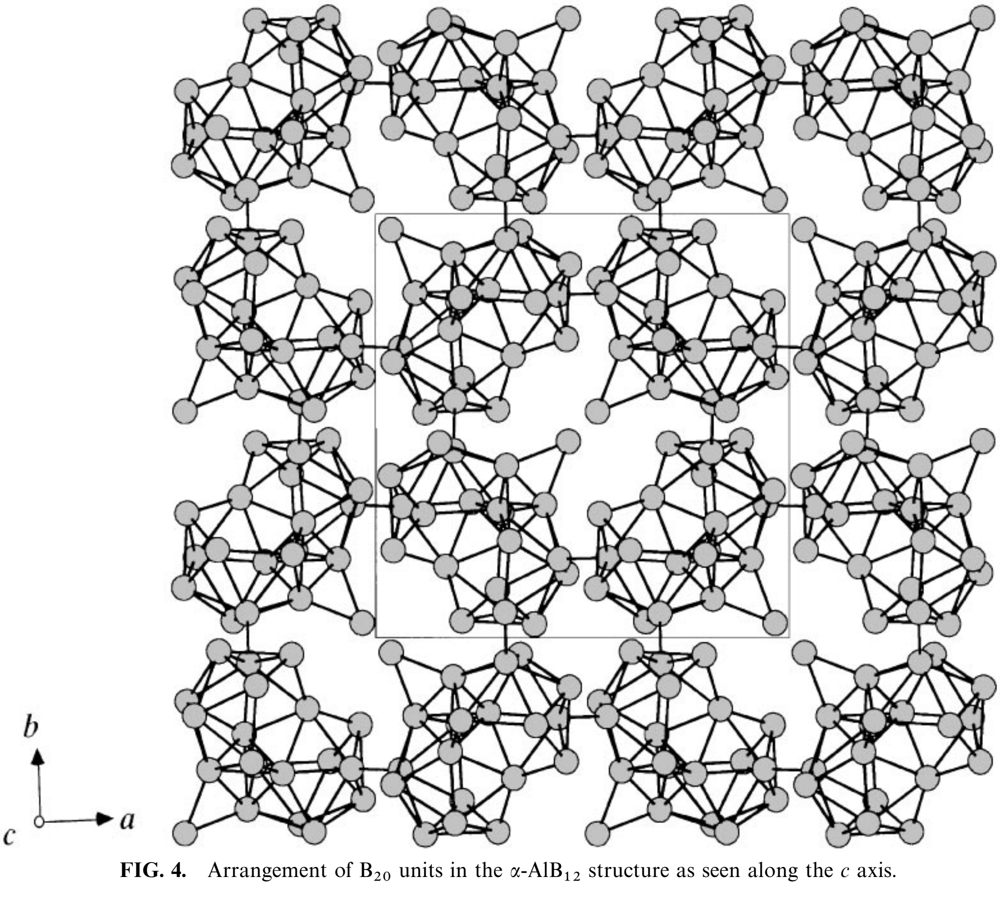

FIG. 4. Arrangement of B_{20} units in the α-AlB_{12} structure as seen along the *c* axis.

seen along the *a* axis is presented in Fig. 5, where four B_{12} icosahedra are arranged in a tetrahedral form; the $4B_{12}$ tetrahedron consists of the B_{12} asymmetric unit in the γ-AlB$_{12}$ structure. By operating the twofold screw axis (of the space group $P2_12_12_1$), which lies at about the center of the $4B_{12}$ tetrahedron in the direction of the *a* axis, the full structure of the icosahedral B_{12} framework can be generated. As a result, two layers of the kagomé nets consisting of interconnected $4B_{12}$ tetrahedra form the basic structure of the icosahedral B_{12} framework. The large openings between two layers have the form of a truncated tetrahedron having a B_{12} icosahedron at each of its 12 apical sites. The B_{20}-(C_2) and B_{20}-(C_s) units fill the large openings, thus linking to 12 B_{12} icosahedra arranged in the truncated tetrahedral form. Detailed descriptions of the coordinations of B_{12} icosahedra surrounding each of the B_{20} units are given in Ref. (11).

A boron network made up of the B_{20}-(C_2) and B_{20}-(C_s) units as seen along the *a* axis is presented in Fig. 6. It consists of B_{20} zigzag chains running along the *c* axis direction. There are two kinds of zigzag chains; one is B_{20}-(C_2) and the other B_{20}-(C_s). Every B_{20} unit within the zigzag chains is linked to a nearest B_{20} unit of different zigzag chains, forming an approximately hexagonal

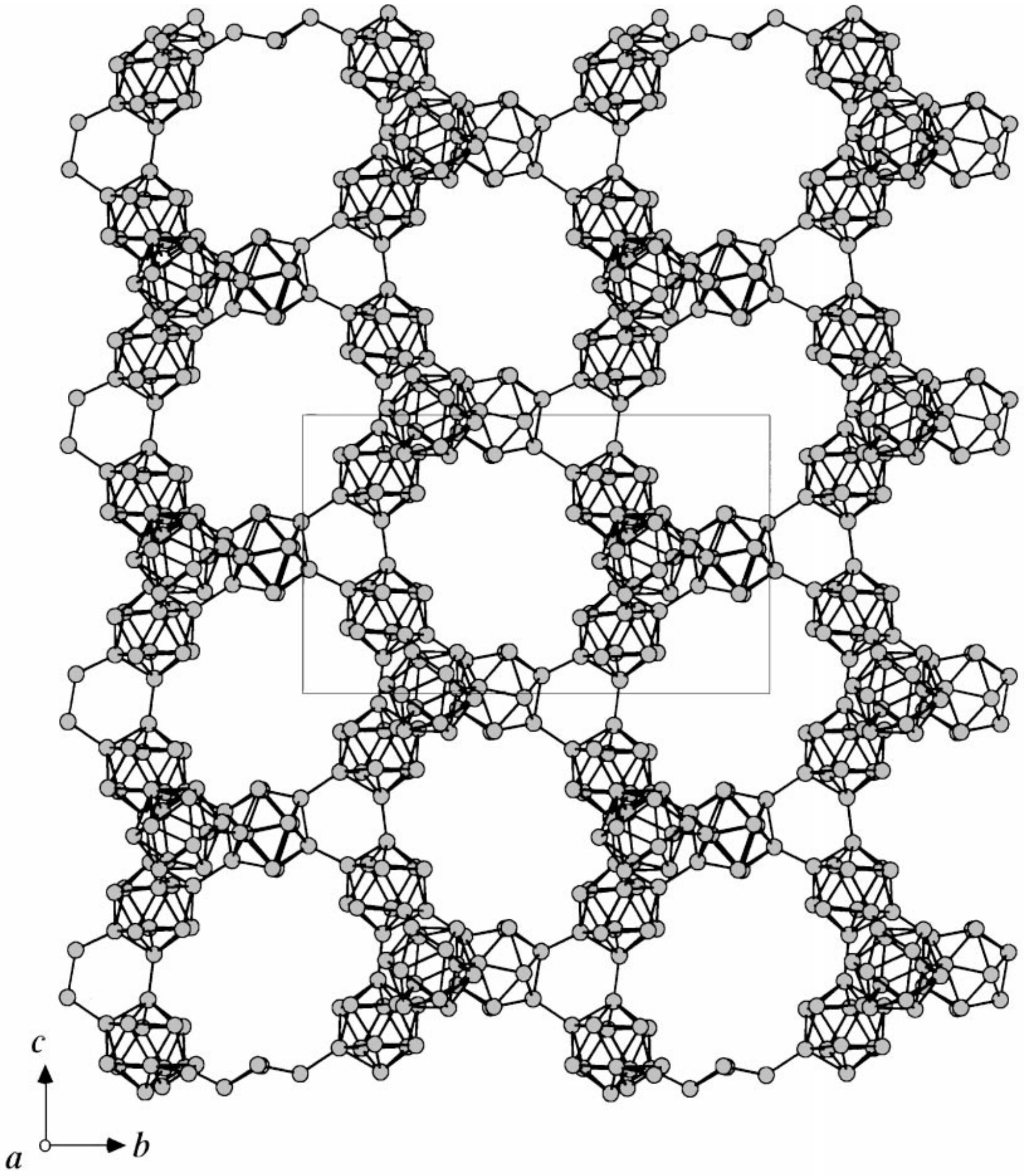

FIG. 5. Arrangement of B_{12} icosahedra in the γ-AlB$_{12}$ structure as seen along the *a* axis.

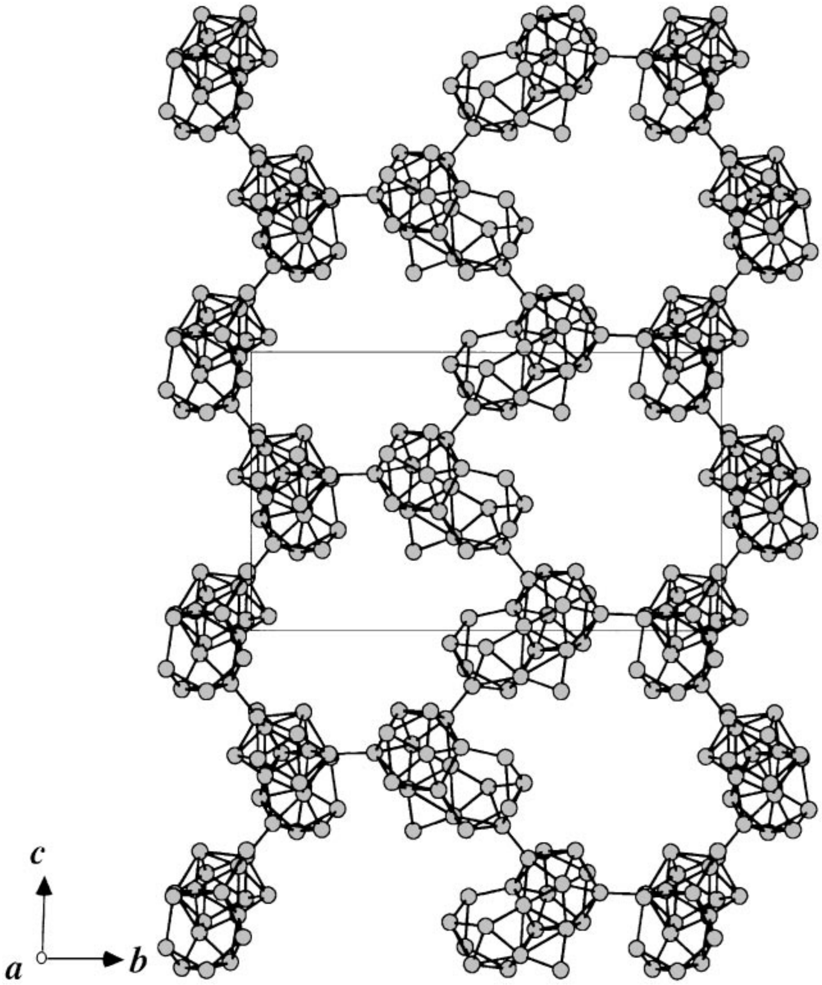

FIG. 6. Arrangement of B_{20} units in the γ-AlB_{12} structure as seen along the *a* axis.

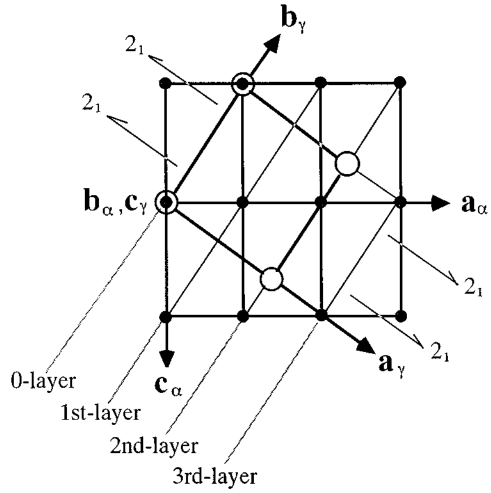

FIG. 7. Relationships of the unit cells or structures of α-AlB_{12} and γ-AlB_{12} in the syntactically intergrown crystal of both phases. Solid black circles represent the lattice points of α-AlB_{12} and the larger white circles those of γ-AlB_{12}. The 2_1 symmetry element is related only to γ-AlB_{12}.

network of B_{20} units. As in the icosahedral B_{12} network, with the 2_1 symmetry axis laying at about the center of each hexagon of the network in the direction of the *a* axis, the full structure of the boron framework of B_{20} units is obtained. As can be expected from the figure, the linkages of the networks in the direction of the *a* axis occur between different types of B_{20} units just as in the *b* axis direction.

2.3. Aluminum Distributions in the Boron Frameworks of α-AlB_{12} and γ-AlB_{12}

The Al atoms are distributed over 5 sites (α-AlB_{12}) or 11 sites (γ-AlB_{12}) which are located outside the B_{12} or B_{20} units. The occupancies of five sites in the α-AlB_{12} structure are respectively 0.72, 0.49, 0.24, 0.15, and 0.02 (8). In the γ-AlB_{12} structure, the occupancies are 0.96, 0.95, 0.95, 0.76, 0.75, 0.52, 0.51, 0.44, 0.19, 0.19, and 0.07, respectively (11). From an electronic point of view, it would

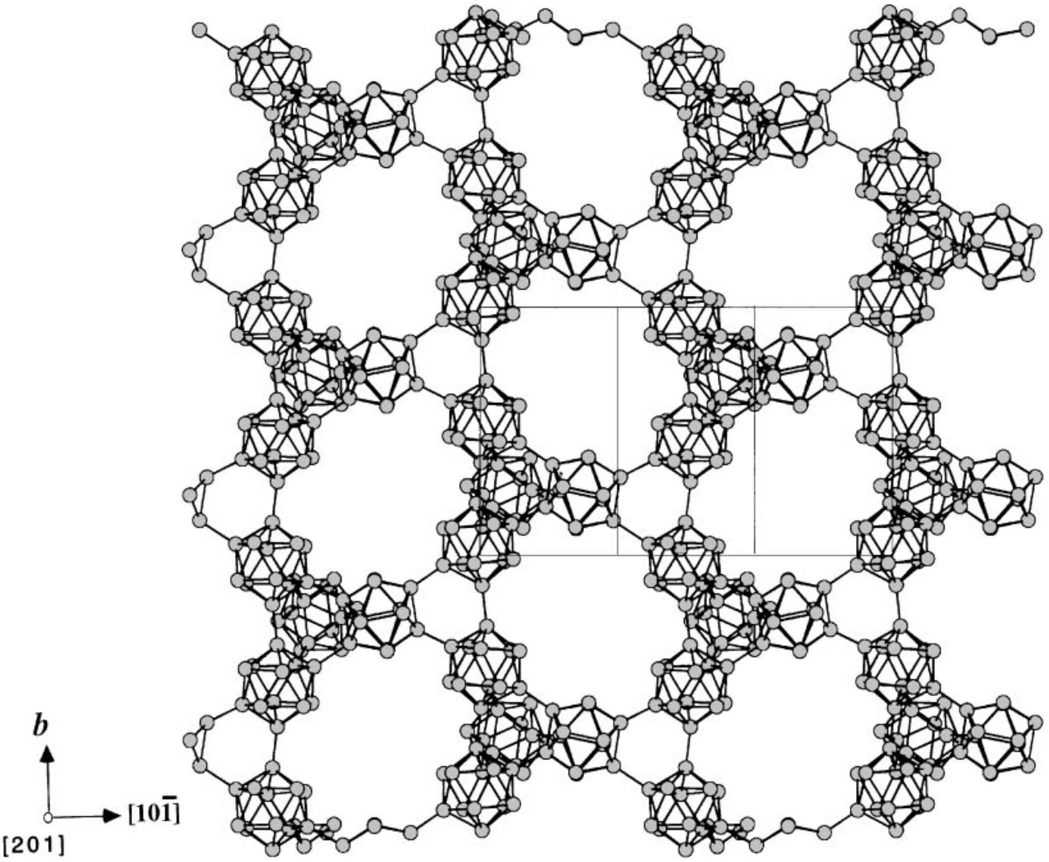

FIG. 8. Arrangement of B_{12} icosahedra in the α-AlB$_{12}$ structure as projected along the (201) axis onto the (101) plane. The (101) unit plane indicated around the center of figure is divided into three equal parts, each of which corresponds to the d_{102} spacing.

be reasonable that the Al atoms are distributed so as to stabilize equally all the B structural subunits (B_{12} and B_{20}), which are considered to be electron deficient. Therefore, charge balance among the boron structural subunits in α-AlB$_{12}$ and γ-AlB$_{12}$ was examined by counting the number of contacts between Al atoms and the boron units (11, 15). The result of the examination indicates that, although distributed in an apparently complicated manner, the Al atoms in the α-AlB$_{12}$ and γ-AlB$_{12}$ phases are distributed in such a way that they preserve a negative charge balance among B_{12} and B_{20} units in a ratio of about 1 : 3, which is probably essential to make up the stable boron frameworks. The results are compatible with the ionic formulas proposed from molecular orbital calculations (11, 14, 15): (10/3) $Al^{3+} \cdot 2B_{12}^{-2}$ B_{20}-$(C_2)^{6-}$ for α-AlB$_{12}$, and (20/3)$Al^{3+} \cdot$ $4B_{12}^{2-}$ B_{20}-$(C_2)^{6-}$ B_{20}-$(C_s)^{6-}$ for γ-AlB$_{12}$.

3. RELATIONSHIP OF THE STRUCTURES OF α-AlB$_{12}$ AND γ-AlB$_{12}$

As mentioned in the Introduction, the crystals of γ-AlB$_{12}$ are obtained as syntactically intergrown crystals with α-AlB$_{12}$. The relationship of the unit cells of both phases in the syntactically intergrown crystals (4) is shown in the Fig. 7. The 2_1 symmetry element in the figure is applicable only to the γ-AlB$_{12}$ structure. In this figure, the unit cell of γ-AlB$_{12}$ is derived by the transformation of the α-AlB$_{12}$ unit cell as shown in the following:

$$\begin{pmatrix} a \\ b \\ c \end{pmatrix}_{\gamma} = \begin{pmatrix} 4/3 & 0 & 2/3 \\ 1 & 0 & -1 \\ 0 & 1 & 0 \end{pmatrix} \begin{pmatrix} a \\ b \\ c \end{pmatrix}_{\alpha}.$$

The B_{12} or B_{20} frameworks of α-AlB$_{12}$ so far presented (Figs. 3 and 4) might seem quite different from those of γ-AlB$_{12}$ (Figs. 5 and 6). It is striking, however, that the B_{12} or B_{20} network of α-AlB$_{12}$ as projected along the (201) axis onto the (101) plane (Fig. 8 or 9) shows the same arrangement of the B_{12} or B_{20} units as that in the γ-AlB$_{12}$ structure (Figs. 5 and 6). The only difference between them is that in the α-AlB$_{12}$ structure the B_{20} framework consists solely of B_{20}-(C_2) units, while in the γ-AlB$_{12}$ structure the

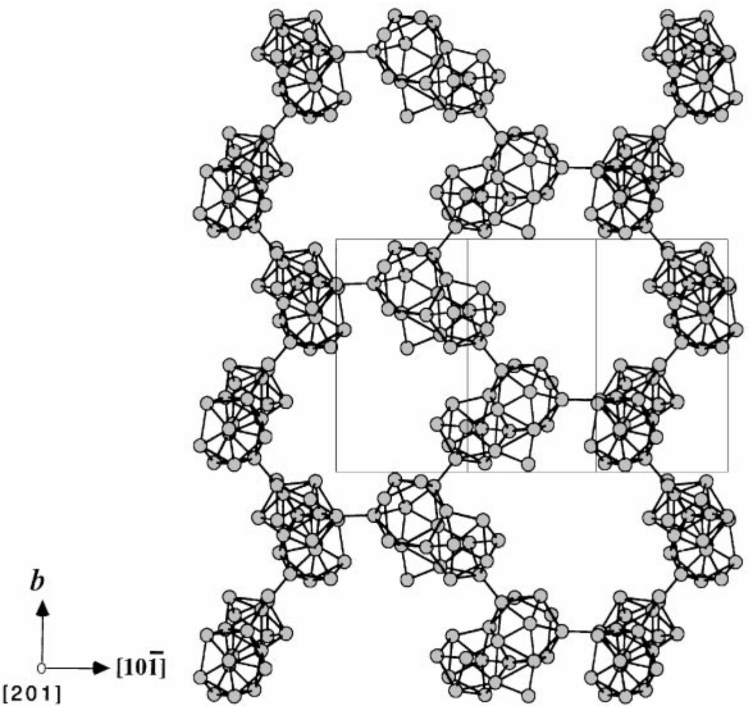

FIG. 9. Arrangement of B_{20} units in the α-AlB_{12} structure as projected along the (201) axis onto the (101) plane. The (101) unit plane indicated around the center of figure is divided into three equal parts, each of which corresponds to the d_{102} spacing.

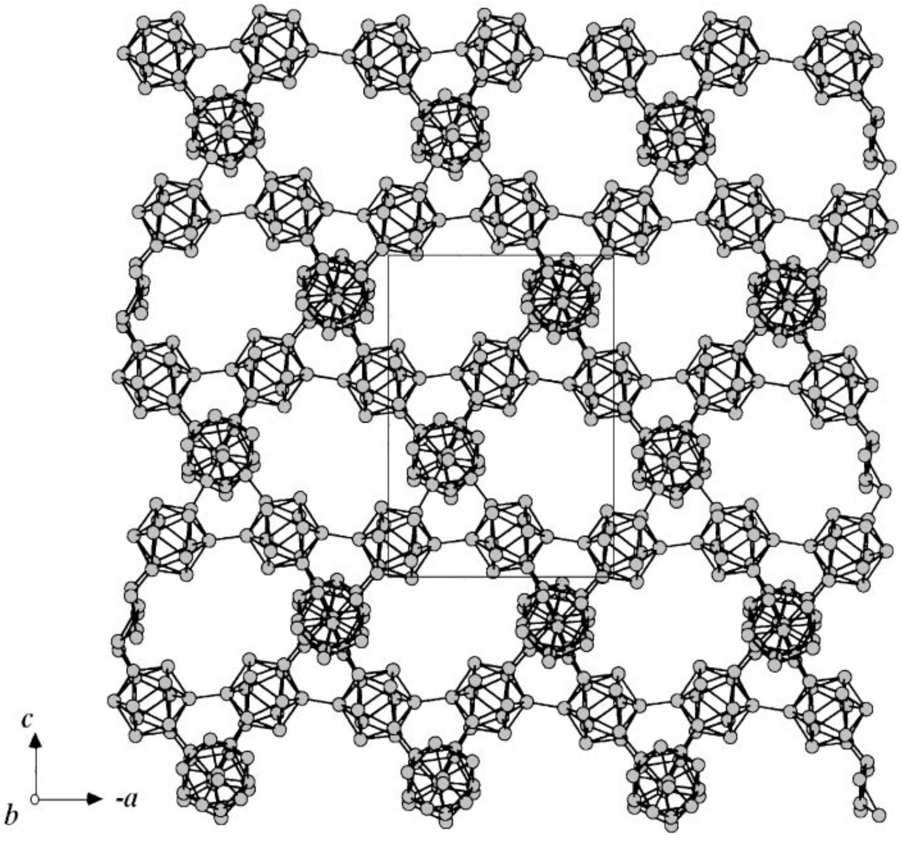

FIG. 10. Arrangement of B_{12} icosahedra in the α-AlB_{12} structure as seen along the *b* axis.

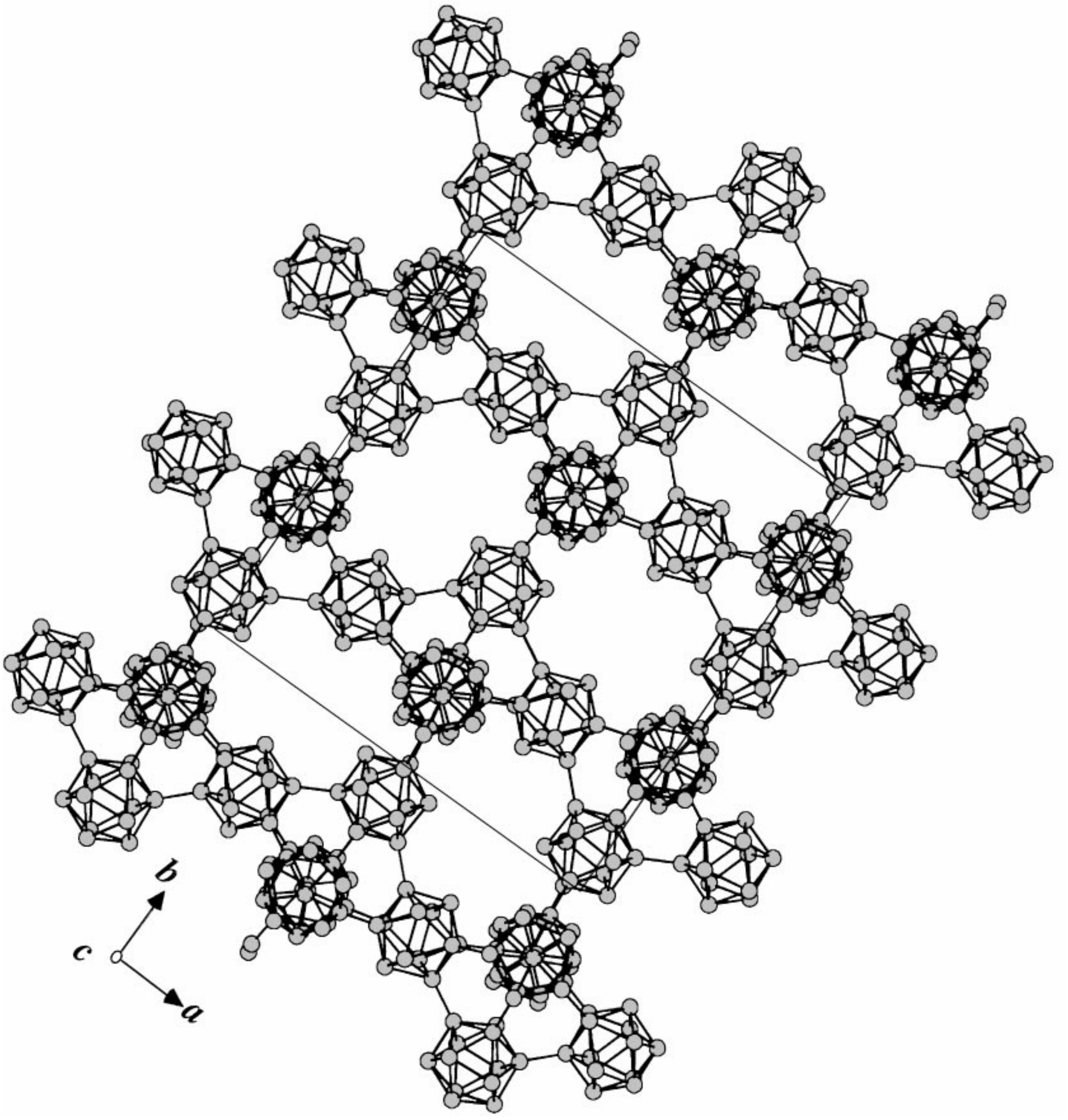

FIG. 11. Arrangement of B_{12} icosahedra in the γ-AlB_{12} structure as seen along the c axis.

B_{20} framework consists of both the B_{20}-(C_2) and B_{20}-(C_s) units. In the intergrown crystal with the relationship shown in Fig. 7, the structure of α-AlB_{12} is constructed by the translation of the B_{12} and B_{20} networks (Figs. 8 and 9) as $(1/2)\, a_\gamma + (1/3)\, b_\gamma$, as well as by the unit translation of the networks along the a_α or c_α axis. On the other hand, the structure of γ-AlB_{12} is generated by operating the 2_1 symmetry operators as indicated in Fig. 7. In the γ-AlB_{12} structure, consequently, the layers (B_{12} and B_{20} networks) with an odd number are those which are generated by the 180° rotation of the basic layer (0-layer or a layer of even number) around the 2_1 axis. In the α-AlB_{12} structure, on the other hand, all the layers lie at crystallographically equivalent planes. This is the fundamental difference in the structures between α-AlB_{12} and γ-AlB_{12}, together with the fact that the B_{20} framework in the former consists of only B_{20}-(C_2) units, while that in the latter consists of both types of B_{20} units.

An icosahedral B_{12} network in α-AlB_{12} (viewed down the b axis) and in γ-AlB_{12} (viewed down the c axis) is shown in Figs. 10 and 11, respectively; they are both parallel with the $(010)_\alpha$ or $(001)_\gamma$ plane of the intergrown crystal as shown in Fig. 7. On first viewing, they might seem to have the same icosahedral B_{12} arrangement. In the α-AlB_{12} structure, however, there are infinite linear chains of icosahedral B_{12} units running along the a axis as seen in Fig. 3, although in the γ-AlB_{12} structure there are no such infinite linear chains running along the corresponding direction.

The difference between the arrangements of B_{12} icosahedral units in these networks reflects the difference of the unit plane areas parallel to these networks (Fig. 7).

As mentioned in the Introduction, the γ-AlB_{12} crystal phase in the pure binary Al–B system displays two unusual natures: First, it is almost always obtained as syntactically intergrown crystals with α-AlB_{12}; and second, by pulverization (to prepare a sample for powder X-ray diffraction), the γ-AlB_{12} phase in the intergrown crystals is transformed into the α-AlB_{12} phase. The close similarity of the B_{12} and B_{20} networks in α-AlB_{12} (Figs. 8 and 9) with those in γ-AlB_{12} (Figs. 5 and 6), which are all parallel with the intergrowth plane $(101)\alpha$ or $(100)\gamma$, may facilitate the formation of the syntactically intergrown crystals.

REFERENCES

1. E. J. Felten, *J. Am. Chem. Soc.* **78,** 5977 (1956).
2. J. A. Kohn and D. W. Eckart, *Anal. Chem.* **32,** 296 (1960)
3. J. A. Kohn and D. W. Eckart, *Z. Kristallogr.* **116,** 134 (1961).
4. J. A. Kohn, G. Katz, and A. A. Giardini, *Z. Kristallogr.* **111,** 53 (1958)
5. V. I. Matkovich, J. Econmy, and R. F. Giese, Jr., *J. Am. Chem. Soc.* **86,** 2337 (1964).
6. I. Higashi, T. Shishido, T. Narukawa, Y. Iimura, T. Sugawara, and T. Fukuda, Paper presented at the ISBB'99, Sept. 5–10, 1999, Dinard, France.
7. I. Higashi, M. Kobayashi, Y. Takahashi, S. Okada, and K. Hamano, *J. Cryst. Growth* **99,** 998 (1990).
8. I. Higashi, T. Sakurai, and T. Atoda, *J. Solid State Chem.* **20,** 67 (1977).
9. J. S. Kasper, M. Vlasse, and R. Naslain, *J. Solid State Chem.* **20,** 281 (1977).
10. R. E. Hughes, M. E. Leonowicz, J. T. Lemley, and L.-T. Tai, *J. Am. Chem. Soc.* **99,** 5507 (1977).
11. I. Higashi, *J. Solid State Chem.* **47,** 333 (1983).
12. I. Higashi and T. Takahashi, *J. Less-Common Metals* **81,** 135 (1981).
13. M. Vlasse, R. Naslain, J. S. Kasper, and K. Plooq, *J. Solid State Chem.* **28,** 289 (1979).
14. T. Ito, I. Higashi, and T. Sakurai, *J. Solid State Chem.* **28,** 171 (1979)
15. I. Higashi, *J. Solid State Chem.* **32,** 201 (1980).
16. I. Higashi, *in* "Boron-Rich Solids" (D. Emin, T. L. Aselage, C. L. Beckel, I. A. Haward, and C. Wood, Eds.), AIP Conf. Proc. 140, pp. 1–10. Am. Inst. Phys., New York, 1986.
17. I. Higashi, H. Iwasaki, T. Ito, T. Lundström, S. Okada, and L.-E. Terginius, *J. Solid State Chem.* **82,** 230 (1989).
18. T. Atoda, I. Higashi, and M. Kobayashi, *Sci. Papers I.P.C.R.* **61,** 92 (1967).